Electroluminescence Characterization of III-V Multi-junction Solar Cells

P. Espinet[*]*, C. Algora, I. Rey-Stolle, I. García and , M. Baudrit*

[1] Instituto de Energía Solar, E.T.S.I. Telecomunicación, Universidad Politécnica de Madrid

pespinet@ies-def.upm.es

ABSTRACT

Characterization is a key process in attaining high efficiency in the state-of-the-art multi-junction solar cells. This work will summarize our efforts in using eletroluminescence for characterising multijunction solar cells. This study will present the possibilities of electroluminescence (EL) spectroscopy as a fast and simple characterization technique which is able to provide extensive information about the solar cell's performance. Finally, four of the applications of this technique will be presented: band gap estimation, barrier effect for minority carriers, information on the thermal performance of encapsulated devices and determination of the shunt resistance of each cell in a dual junction device.

Index Terms: Electroluminescence; Multi-junction Solar Cells; Characterization.

INTRODUCTION

III-V multijunction solar cells are complicated photovoltaic devices which issue great challenges in terms of device characterization. EL has the advantages of being non-destructive, no needs of special sample preparation and the set-up is extremely simple. This makes it a fast and simple characterization technique able to provide valuable information about the manufacturing process. Faster and more economic techniques of characterizing multi-junction solar cells may become increasingly important in the industry and EL could play an important role in this. The use of EL measurements in solar cells is by no means new. However, EL has not been widely used, indeed most of the EL applications have not been shown yet. In this report, several EL utilities are discussed with measurements of GaInP single junction solar and GaInP/GaAs dual junction solar cells.

THEORETICAL BACKGROUND

EL is the phenomenon in which a PN junction emits light in response to an electric current that is passed through it, when the carriers injected recombine in a radiative process. The most common radiative transition in semiconductors is between states in the conduction and the valence bands. The spontaneous emission rate r_{sp} (ε) is defined in [1]:

$$r_{sp}(h\nu) \approx \left[1 - f_v(E_1)\right] \cdot f_c(E_2) \cdot N_J(h\nu) \cdot P_{em} \qquad (1)$$

where

- E_1 is the energy of the hole and E_2 is the energy of the electron and $(E_2 - E_1) = h\nu$.the energy of the emitted photon.
- f_v , f_c is the probability that a state in the valence band or in the conduction band is occupied respectively.
- N_J $(h\nu)$ is the density of states with a state in the conduction band filled and a state in the valence band empty, the joint density of states.
- P_{em} is the emission probability.

To produce emission it is necessary that the PN junction is not in equilibrium. Next consider the case of weak injection, such that the quasi-Fermi levels are still several k_BT away from the bandedges and are within the bandgap. For parabolic electron-hole bands the spontaneous emission has the following expression,

$$r_{sp}(h\upsilon) = \frac{\left(2m_r^*\right)^{3/2}}{2\pi^2 \mathrm{h}^3 \tau_{rad}} (h\upsilon - E_g) e^{-h\upsilon/k_BT} \sqrt{h\upsilon - E_g} \qquad (2)$$

Where m_r^* is the reduced mass, τ_{rad} the radiative lifetime, $h\nu$ the energy of the emitted photon, E_g the bandgap of the solar cell material, k_B Boltzman's constant and T the absolute temperature.

Equation (2) reveals the following facts:

- The gap energy is the lowest limit where the EL goes to zero
- The maximum EL intensity is obtained by deriving equation (2) and occurs when the energy is greater than E_g, in particular:

$$E_{EL\max} = E_g + \frac{k_BT}{2} \qquad (3)$$

The peak in the density distribution of electrons in the conduction band occurs at an energy $k_BT/2$ above the band minimum. Therefore, the band-to-band transition energy is slightly larger than E_g.

- The EL peak has a determined width resulting from the thermal distribution of the carriers in the bands, the so called *thermal broadening* of the EL. The full width at half maximum follows the relation [2]:

$$FWHM_{EL}(eV) = 1.8k_BT \qquad (4)$$

However, the linewidth of the spontaneous emission spectrum is determined by various line-broading mechanism apart from the thermal broading. These can be classified into homogeneous and inhomogenous line-broading mechanisms. Homogenous broading occurs mainly due to phonon interactions and all parts of the gain medium are affected uniformly. Inhomogeneous broading is due to

978-1-4244-1641-7/08/$25.00 ©2008 IEEE

local variations of the electronic properties accross the sample. In this case only selected parts are affected. Inhomogeneous contributions arise from localized strain, impurity density variations, alloy clustering, interface roughness in heterostructures.

EXPERIMENTAL

Set-up

The set-up used for EL measurements consists of the following elements:

- A high precision current source (HP4142B)
- Collimator
- Optical Spectrum Analyzer (Spectra 320)
- Computer

We control the current injected into the solar cell with the current source. The light is directed towards the collimator coupled to the fiber optic of the spectrometer. The objective of the collimator is to achive a greater numerical aperture. The testing device is placed on an x-y-z positioner. The solar cell is moved to find the point of maximum detection. Once the solar cell is correctly positioned measurements at different injected currents can be taken. The spectrum of the emitted light is detected with a spectrometer that is connected to a computer. The computer processes and displays the results.

Solar cell manufacture

Some EL applications are presented in detail within this paper, for which GaInP top cells and GaInP/GaAs dual junction solar cells were fabricated. These semiconductor structures were grown by low pressure-Metal Organic- Vapor Phase- Epitaxy (MOVPE). Once grown, the structures were processed into $1mm^2$ solar cells following a manufacturing strategy close to that of optoelectronics and is described in detail elsewhere [4], [5]. The main characteristics of the cells are:

- Front grid definition by photolithography with a shadowing factor of 5%.
- Front and back metallic contacts by Joule-effect metal evaporation.
- Devices on a wafer were isolated by means of a mesa etching.
- Assembling and encapsulation: wire bonding for the front side, solder paste for the back side.

APPLICATIONS

Band gap determination

The band gap of $GaInP_2$, is a function of numerous growth conditions that range from 1.8 to 1.9 eV [6], [7]. The position of the EL maximum is related to the band gap according to equation (3). In this paper, the band gap of the top cells is determined directly from the EL measurement. The band gap of each top cell has also been obtained by External Quantum Efficiency (EQE). In this case, the band gap was determined by a linear fitting in the EQE for the low energy side of the curve. Table 1 summarizes the results about gap energy.

Top Cell	Band gap_{EL} ±0.24(nm)	Band gap_{EQE} ±0.5(nm)	Band gap_{EQE}- Band gap_{EL} ±0.75(nm)	Difference (%)
#1	668.06	675.21	7.15	1
#2	680.34	694.95	14.61	2.1
#3	678.79	694.06	15.27	2.2
#4	681.11	692.75	11.64	1.7

Table 1. Bandgap determination by EL and by EQE

Note the slightly higher (wavelength) bandgap is determined by EQE with a difference lower than 2.3%. This difference is mainly due to the first approximation of the calculation of the band gap by a linear fitting in the EQE. On the other hand, in this case the band gap is highly sensitive to the points taken in the adjustment and the characteristics of the base. Then, EL is a faster and more systematic and repetitive method than EQE in determining the band gap.

Barrier effect for minority carriers

An effective back surface field (BSF) is a key structural element for any subcell in a high-efficiency multi-junction concentrator solar cell. The design of optimum BSF layers for top cells has received some attention [8,9], and AlGaInP layer has been reported as one of the best option.

We studied the back surface passivation of the $GaInP_2$ solar cells for future $GaInP_2$/GaAs dual junction solar cells. The $GaInP_2$ top cell must be made very thin because of the requirement of current matching of the top and bottom cell. Therefore, the back surface field has a significant effect on the short-circuit current of the thin top cell.

Two similar structures but with different BSF layers have been used in this study. We examinated the diferences between two thicknesses.

Structure	#5	#6
Material	AlGaInP	AlGaInP
Doping	$6*10^{17}$ cm^{-3}	$6*10^{17}$ cm^{-3}
Thickness	75nm	45nm

Table 2. Characteristics of the different BSF layers compared in this study.

Figure 1 shows the EL spectrum for this two structures for a low injected current of 10 mA. The top cell #6 presents an additional peak of emission corresponding to the GaAs buffer layer. While the top cell #5 just presents a single peak of emission corresponding to the $GaInP_2$.

In order to explain these experimental results, some simulations with Silvaco ATLAS® have been done.This advanced simulator is capable of calculating accurately the bands diagram of the heterojunction involved. The potential of this software package to evaluate the performance of III-V multi-junction solar cells has been recently pointed out [10].

978-1-4244-1641-7/08/$25.00 ©2008 IEEE

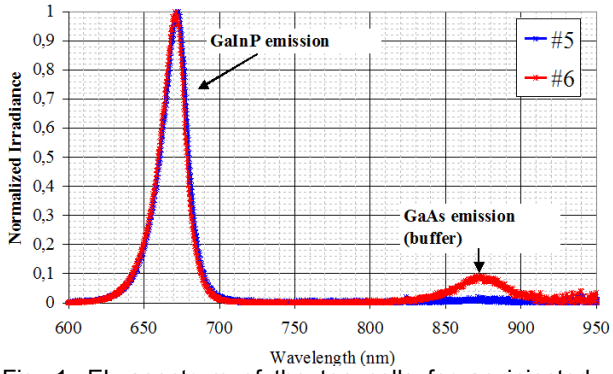

Fig. 1. EL spectrum of the top cells for an injected current of 10 mA.

The bands diagram of the base, BSF and the buffer layers depicted in figure 2, helps to understand the experimental and the simulation results. Both buffer layers are p-type so the minority carriers are electrons, thus they are responsible for the radiative recombination and consequently light emission. The conduction band of the BSF in top cell # 5 makes a potential barrier for the electrons being unable for them to reach the buffer to recombine. However, BSF in the top cell #6 shows a very poor reflection for minority carriers. Then, there is an injection of electrons in p-type GaAs buffer where they recombine.

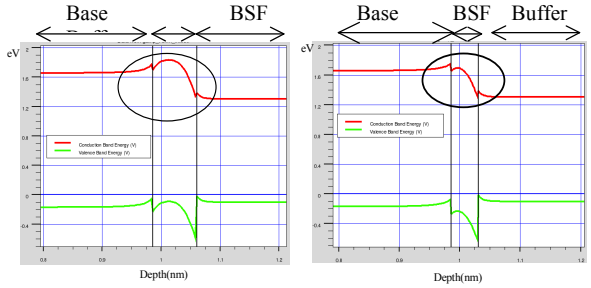

Fig. 2. Bands diagram of the base, the BSF and the buffer. of top cell #5(left diagram) and top cell #6 (right diagram)

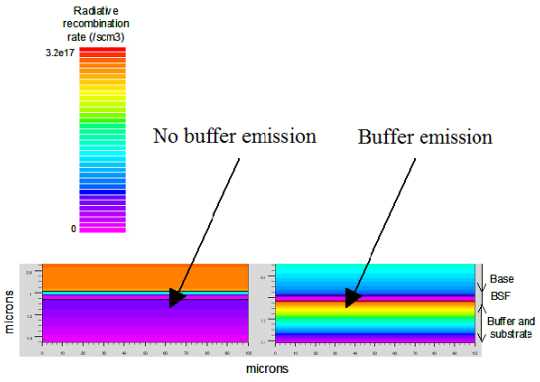

Fig. 3. False color map of the radiative recombination rate. Left structure corresponds to the top cell #5 and the right structure represents the top cell #6

Figure 3 depicts a map in false color of the radiative recombination simulation of the two cases. One with intense GaAs emission (top cell # 6), and the other, the top cell which does not present the additional GaAs emission peak (top cell #5). As it can be seen in figure 3, top cell #6 presents an intense radiative recombination in the buffer region (GaAs) while in top cell # 5 the radiative recombination in the buffer area is negligible as it was shown in the experimental measurements of figure 1.

Then, in this experiment we prove the possibility of comparing with EL the barrier of the BSF for minority carrier. We are currently studying the impact of these results in the design of an optimal BSF for solar cells.

Thermal performance of encapsulated devices

The junction temperature in a solar cell is a critical parameter for two reasons. First, the solar cell performance depends on the junction temperature. Second, high temperature operation shortens the device´s lifetime [12]. Given this, it is necessary to encapsulate the cell to a heat sink able to work at the desired concentration. Here, EL is a very helpful tool in providing information about the thermal performance of the encapsulated solar cells. Two solar cells of type #5 (table 2) were encapsulated, one on a copper plate (good heat removal) and the other on a ceramic plate (alumina, moderate heat removal). According to equation (3), when the device is biased at different currents, any shift detected in maximum of EL will reflect changes in the temperature of the junction.

The solar cells used in this study (size 1mm^2) are designed for operating at 1000X. Assuming an efficiency of 30%, 0.3W is converted into electricity while 0.7W is transformed into heat. Then, the task of the sink is the heat extraction of 0.7W. Therefore, the electrical power supplied to the cell for the EL measurements is 0.7W.

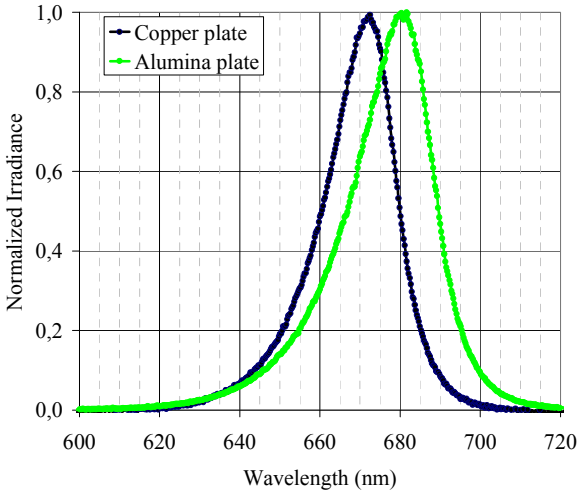

Fig.4 EL spectrum for the GaInP solar cell enacapsulated in two different plates for an inyection of 0.7W

The results of the comparison between the good and the moderate sink are presented in table 3. As can be seen in the column corresponding to the cell encapsulated on copper, there is a small shift in the EL

978-1-4244-1641-7/08/$25.00 ©2008 IEEE

peak indicating good heat removal capabilities, as expected. On the other hand, for alumina encapsulated devices an evident shift in the EL peak towards higher wavelengths is observed (figure 4). This shift is translated into temperature changes at the junction. These results are shown in the last column of table 3 (using eq. 3). In summary, with a simple EL experiment the performance of a given encapsulation can be easily assessed by simple comparative experiments.

Electrical Power (W)	λmax_{EL} copper plate ±0.24(nm)	ΔT (ºC) copper plate ±3ºC	λmax_{EL} alumina plate (nm) ±0.24(nm)	ΔT (ºC) alumin a plate ±3ºC
0.7	679.27	13	681.65	61

Table 3. Wavelengths where the maximum EL occurs in cells with good or moderate heat removal.

Detection of low shunt resistance in a multi-junction solar cell

A dual junction solar cell consists of two junctions of different materials connected in series. Therefore, in a GaInP/GaAs dual junction when forward biased, two peaks will be obtained each one corresponding to the EL emission of each junction (see figure 5). Roughly, the GaAs subcell should start emitting when it reaches a voltage over ~0.9 V. However, the GaInP junction needs ~1.3 V to emit [3].

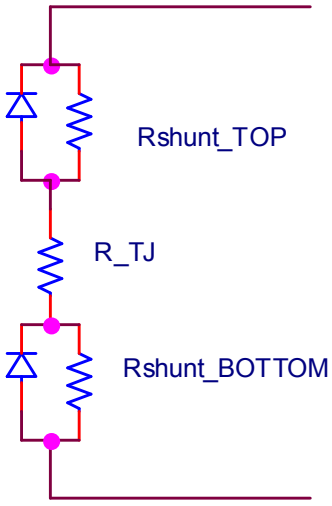

Fig.5. Equivalent circuit of a dual junction solar cells for EL analysis

However, sometimes only one of the junctions emits. The figure 6 shows a case in which only emits the bottom cell. We think that the top cell has such a low shunt resistance, that it is unable to reach the 1.3V required to start emitting. This assumption was corroborated by other measurements like EQE and I-V curve.

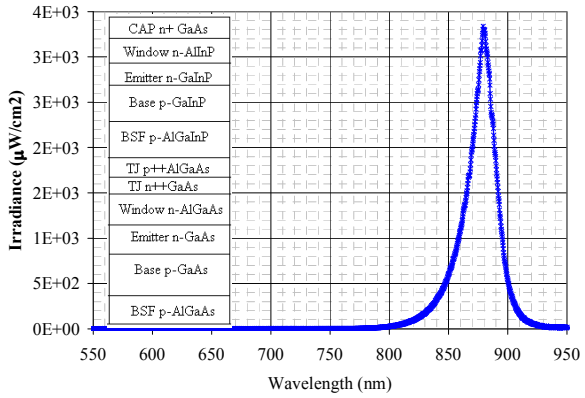

Fig.6. Emission spectrum for an injection of 150mA in a dual junction solar cell with low shunt resistance in the top cell

The procedure followed for measuring EQE of a dual junction solar cell was:

- For the top cell, a 800 nm laser was employed to flood the bottom cell and to make the top cell limit the current.
- For the bottom cell the procedure is similar but a 620 nm laser was used to flood the top cell.

An accurate bias to bring the subcell measured to its short circuit regimen should be needed. As it has been reported [11] differences in the EQE when biasing the subcell can reveal wide variety of problems. In the case of the top cell, different bias is translated into a variation of level in all the wavelengths (figure 7). Then, it means a low shunt resistance in the top cell measured. On the other hand, we can see that the bottom cell is virtually independent of the bias level.

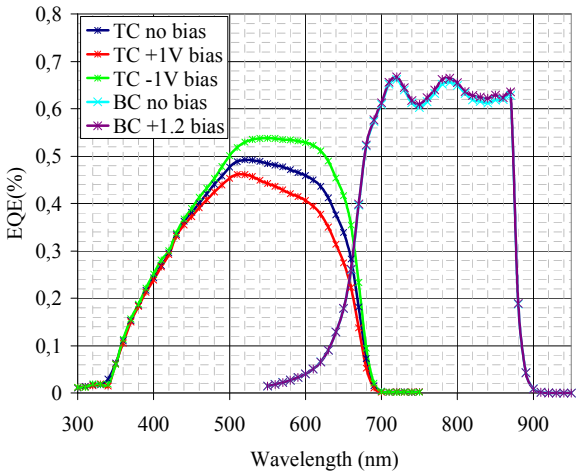

Fig.7. EQE of the dual junction solar cell with low shunt resistance in the top cell.

The problem of a low shunt resistance is also seen in the I-V curve at one sun, presenting a no flat curve in the vecinity of short-circuit (figure 8). However with this measurement it is impossible to distinguish which junction has the shunt resistance problem or even if

978-1-4244-1641-7/08/$25.00 ©2008 IEEE

both junctions have problems. Therefore, EL is an useful tool in order to discern which junction has the problem.

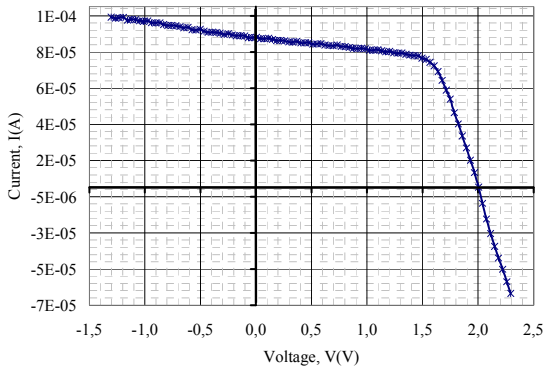

Fig. 8. I-V curve od the dual junction solar cell at 1 sun.

At a considerably high enough current the voltage drop in the shunt resistance of the top cell reaches the emission threshold, so top cell starts to emit. A picture of this solar cell emitting at 400 mA is showed in the figure 9. It can be seen in the photo that even for this high injected current, there are some areas where the shunt resistance is so low that the junction does not emit.

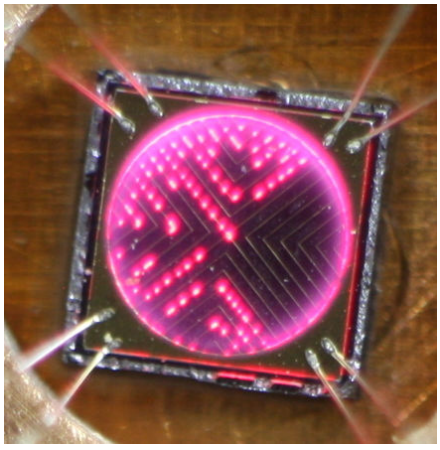

Fig. 9. EL emission of a dual junction solar cell of this study for an injection current of 400mA.

A similar procedure can be established in order to detect shunts on the bottom cell.

CONCLUSIONS

We showed in this paper that EL as a characterization tool for multijunction solar cells has a great potential to be developed. A study of some EL applications for solar cells has been presented. We showed that important aspects of the solar cell can been determined with EL. Some examples of these possibilities have been provided: band gap estimation, barrier effect for minority carriers, information on the thermal performance of encapsulated solar cells and information on the shunt resistance of each cell in a dual junction solar cell.

ACKNOWLEDGMENT

This paper has been supported by the European Commission under contract SES6-CT-2003-502620 (FULLSPECTRUM
project). The Spanish Ministerio de Educación y Ciencia has also contributed with the CONSOLIDER-INGENIO 2010 program by means of the GENESIS FV project (CSD2006-004) and also with the research projects with references TEC2005-02745 and TEC2004-22300-E. The Comunidad de Madrid has also contributed under NUMANCIA programme (S-05050/ENE/0310) . Pilar Espinet is holds a scholarship from the Comunidad de Madrid

7. References

[1] P. Bhattacharya, "Semiconductor Optoelectronic Devices*",* 2nd Edition, Prentice Hall, 1998

[2] O. Wada, S. Yamakoshi, H. Hamaguchi, T. Sanada, Y. Nishiutani nad T. Sakurai "Performance and Reliability of High Radiance InGaAsP/InP DH LED´s Operating in the 1.15-1.5 μm Wavelenght Region" IEEE Journal of Quantum Electronics, VOL. QE-18, NO.3, March 1982

[3] H. Yoon, R. R. King, G. S. Kinsey, S. Kurtz, and D. D. Krut "Radiative Coupling Effects in GaInP/GaAs/Ge Multijunction Solar Cells", 3rd World PVSEC, 2003 Osaka, JapanT

[4] C. Algora, I. Rey-Stolle, B. Galiana, J.R. González, M. Baudrit and I.García 2005 "III-V Concentrator Solar Cell as LEDs" Proc. of the 20th EU PVSC, Barcelona, Spain, pp.82-85

[5] C. Algora, I. Rey-Stolle, B. Galiana, J.R. González, M. Baudrit and I.García 2006 "Strategic Options for a LED-Like Approach in III-V Concentrator Photovoltaics" Proc. of the 2006 IEEE 4th World PVSEC Waikoloa, Hawai, pp. 741-744

[6] S.R. Kurtz, J.M. Olson and A.E. Kibbler, Appl. Phys. Lett., 57, 1922 (1990)

[7] A. Gomyo, T. Suzuki and S. Iijima, Phys. Rev. Lett., 60, 2645 (1988)

[8] D.J. Friedman, S.R. Kurtz, K.E. Kibbler, J.M. Olson, Back surface fields for $GaInP_2$ solar cells. In: Proceedings of the 22nd IEEE Photovoltaic Specialist Conference, vol.1, 1991, pp. 358-360.

[9] H. Kurita, T.Takamoto, E.Ikeda, M. Ohmori, "High-efficiency monolithic InGaP/GaAS tandem solar cells with improved top-cell back-surface-field layers". In: Proceedings of the International Conference on Indium Phosphide and Related Materials, 1995, pp. 516-519.

[10] M.Baudrit and C.Algora "Modeling of GaInP/GaAs Dual-junction solar cells including tunneling

models“ Proceedings of the 33rd IEEE Photovoltaic Specialist Conference.
[11] I.García, I.Rey-Stolle, B.Galiana and C. Algora. “Specific growth and characterization issues in multi-junction solar cells for concentrations above 1000 suns”.
[12] M. Vázquez, C.Algora, I. Rey-Stolle, J. R. González “III-V concentrator solar cell reliability prediction based on quantitative LED reliability data”, Progress in Photovoltaics: Research and applications, vol. 15, 2007, pp.477-491

978-1-4244-1641-7/08/$25.00 ©2008 IEEE